# Oxygen Mediated Oxidative Couplings of Flavones in Alkaline Water

Xin Yang[1], Sophie Hui Min Lim[1], Jiachen Lin[1], Jie Wu[2,3], Haidi Tang[2,3] Fengyue Zhao[4], Fang Liu[4], Chenghua Sun[5], Xiangcheng Shi[2], Yulong Kuang[2], Joanne Yi Hui Toy[1], Ke Du[1], Yuannian Zhang[1], Xiang Wang[1], Mingtai Sun[1], Zhixuan Song[1], Tian Wang[2], Ji'en Wu[2], K. N. Houk[*6], Dejian Huang[*1,3]

**Affiliations:**

[1] Department of Food Science and Technology, National University of Singapore, 2 Science Drive 2, Singapore 117542, Republic of Singapore.

[2] Department of Chemistry, National University of Singapore; 3 Science Drive 3, Singapore, 117543, Republic of Singapore.

[3] National University of Singapore (Suzhou) Research Institute; 377 Linquan Street, Suzhou, Jiangsu 215123, China.

[4] College of Sciences, Nanjing Agricultural University; Nanjing 210095, China.

[5] Department of Chemistry and Biotechnology, and Centre for Translational Atomaterials, FSET, Swinburne University of Technology; Hawthorn, Victoria 3122 Australia.

[6] Department of Chemistry and Biochemistry, University of California, Los Angeles; CA 90095, USA.

*Corresponding authors. Email: houk@chem.ucla.edu (K. N Houk) and dejian@nus.edu.sg (Dejian Huang)

**ABSTRACT**

***Catalyzed* oxidative C-C bond coupling reactions play an important role in the chemical synthesis of complex natural products of medicinal importance. However, the poor functional group tolerance renders them unfit for the synthesis of naturally occurring polyphenolic flavones. We have found that molecular oxygen in alkaline water acts as a hydrogen atom acceptor and oxidant in *catalyst-free* (without added catalyst) oxidative coupling of luteolin and other flavones. By this facile method, we have achieved the synthesis of a small collection of flavone dimers and trimers including naturally occurring dicranolomin, philonotisflavone,**

**dehydrohegoflavone, distichumtriluteolin, and cyclodistichumtriluteolin. Mechanistic studies using both experimental and computational chemistry uncovered the underlying reasons for optimal pH, oxygen availability, and counter-cations that define the success of the reaction. We expect our reaction opens up a green and sustainable way to synthesize flavonoid dimers and oligomer using the readily available monomeric flavonoids isolated from biomass and exploiting their use for health promotion and treatment of diseases.**

## INTRODUCTION

Flavonoids constitute a class of plant secondary metabolites that are ubiquitous and diverse in structural variations that have broad bioactivity for human health. The flavonoid core structure features a 15-carbon phenyl-chromone motif and is a privileged structure for drug discovery[1,2]. The structural diversity of flavonoids stems from variable substituent positions of the phenyl, variable numbers and positions of phenol groups on the aromatic rings, number and degree of glycosylation, and formation of flavonoid dimers and oligomers. Flavonoids are known to promote human health not only by reducing the risk factors of non-communicable diseases, including chronic inflammation [3], hypertension[4], diabetes[5], cognitive impairment[6], and diarrhea (Crofelemer)[7], but also combating infectious diseases such as anti-urinary tract infection by A-type proanthocyanidins in cranberry [8] and potential antivirus (SARS-CoV-2) activity of amentoflavone (3′-8-biapigenin) and its derivatives[9], which are active compounds in *Ginkgo biloba* (the oldest tree on the Earth). While flavone monomers are relatively abundant in fruits and vegetables and can be extracted on an industrial scale from agri-food byproducts, flavonoid dimers and oligomers are minor components in plant biomass, and it is not economical to obtain them in a large scale from natural sources. Synthetically,

55 catalyzed C-C bond coupling reactions, [10,11] such as Ullman reaction[12], and Suzuki-
56 Miyaura coupling[13] have been employed (**Fig. 1**) in order to make a limited number of
57 biflavones with moderate overall yields. These high-temperature reactions suffer from
58 major drawbacks due to the usage of toxic heavy metals, wasteful halogens and boronate
59 by-products, and the requirement of protective groups for phenolic functional
60 groups[14,15,16]. Therefore, these methods fail to meet the stringent requirement of green
61 chemical synthesis demanded by sustainable development[17]. Furthermore, the synthesis
62 of triflavonoids remained as unexplored territory.

63

64 We now report a novel *catalyst-free* oxidative coupling reaction of two $sp^2$ C-H bonds of
65 flavones mediated by dissolved molecular oxygen as a hydrogen atom acceptor.
66 Conducted at room temperature and food grade media (alkaline water), our reaction
67 features high yield and good regioselectivity (**Fig. 1c**). By this simple method, we
68 achieved the synthesis of a large number (> 40) of biflavones and triflavones including
69 complex natural products such as dicranolomin, philonotisflavone, dehydrohegoflavone
70 B, distichumtriluteolin, and cyclodistichumtriluteolin found in mosses, one of the oldest
71 land plants.[18] Our discovery is a breakthrough for synthesis and for the exploitation of the
72 great potentials of these compounds as pharmaceutical agents and advanced functional
73 materials.

74 **RESULTS**

75 Hydroxyl group rich flavones (e.g., luteolin) are good reducing agents and have been
76 well-known as potent dietary antioxidants in scavenging biologically relevant reactive
77 oxygen species[19]. Moreover, under alkaline conditions, many weakly acidic flavones
78 including luteolin undergo deprotonation to phenolates, which are sensitive to oxidation

by molecular oxygen to their respective ortho-semiquinone anion radicals that have been detected by electron spin resonance spectra[20,21]. Nevertheless, the fates of these radicals are unknown. We envisioned that these electron-deficient semiquinone radicals may react with electron-rich flavonoid anions by radical-nucleophile coupling. To verify this, we conducted HPLC analysis of the alkaline solution of luteolin (pH 11.5) and indeed found several products (**Supplementary Fig. 1**), which were further characterized as luteolin dimers and trimers by LC-MS. By using the optimal conditions, we scaled the reaction up with 10 gram luteolin and successfully synthesized in one-pot, for the first time, **2a** (42%, Lu-(2′-6)-Lu[22], philonotisflavone (**2a′**, Lu-(2′-8)-Lu, 1.2%), dehydrohegoflavone B (**2a″**, Lu-(6′-6)-Lu, 1.0%). and distichumtriluteolin (**3a**, Lu-(2′-6)-Lu-(2′-6)-Lu, 10%) (**Fig. 2 and Supplementary Fig. 1-3**). These compounds were originally isolated from moss, one of the oldest land plants, particularly *Rhizogonium distichum* which contains all four triluteolin regioisomers including bartramiatriluteolin, strictatriluteolin, and rhizogoniumtriluteolin.[18] Their biosynthesis is likely mediated by enzymes (such as polyphenol oxidase) under the neutral physiological pH of moss. High contents of flavonoids in moss (as high as 10% of its dry weight) were suggested to protect the plant from biotic (e.g. fungi) and abiotic stress (temperature, water, reactive oxygen species, and UV-light)[23,24]. Product **3a** was characterized by high resolution MS, $^{1}H$ and $^{13}C$ NMR spectra, which reveal the existence of atropisomers due to the hindered rotation of interflavonyl bonds[25], such isomerism is common in complex natural products including tryptorubin A[26].

*Cyclodistichumtriluteolin*. Triluteolins such as **3a** have one B ring and one A ring on the terminal luteolin units, respectively, that are close to each other for intramolecular oxidative coupling (**Fig. 2b**). By dissolving **3a** in alkaline water (pH 12.5) at room

temperature overnight, three major cyclotriluteolins, **4a**, **4a′**, and **4a″**, were formed together with some luteolin monomer and **2a** were observed by HPLC in the reaction mixture (**Supplementary Fig. 4**). Apparently, interflavonyl bond isomerization has occurred under the reaction conditions and the expected $(2'\text{-}6)_3$-triluteolin isomer was not detected. The interflavonyl bond cleavage would explain the formation of **1a** and **2a**. These cyclotriluteolins are regioisomers of naturally occurring cyclobartramiatriluteolin ($(2'\text{-}8)_3$ interflavonyl bonds) isolated from moss[27]. To confirm the structure of **4a**, we grew single crystals from its methanolic solution and determined the molecular structure shown by the ORTEP plot (**Fig. 2c)**, which shows the structure to be **4a′** instead of the expected **4a**. The structure of **4a′** adopts a triangular shape with each corner occupied by B rings of the luteolin and the three edges were fenced by the benzopyranyl moieties (with a length of 7.845 Å) forming a hydrophobic cavity with an opening of ~ 6.228 Å. The C(4)=O and C(5)-OH form intramolecular hydrogen bond and the benzopyranyl plane tilts with a dihedral angle of about 70 deg with the plane coincident with the paper surface. In the solid state, **4a′** molecules form hydrophobic channels with hydrophilic OH groups (C(7)OH, C(3′)-OH and C(4′)-OH) pointing outward and C(4)=O and C(5)-OH edge pointing inward. With its unique shape and phenolic groups, cyclotriluteolins may complex guest molecules and metal ions. Thus, it is an intriguing building block for the construction of a functional covalent organic framework (COF).

*Isomerization of Cyclotriluteolin*. In solution, cyclobartramiatriluteolin exhibited one set of the $^{1}H$ and $^{13}C$ NMR spectral peaks for three luteolin units. Due to the $C_3$ axis in **4a**, its $^{1}H$ NMR spectrum agrees with magnetically equivalent luteolin units $C(sp^2)$-H at 25 $^{o}C$ (**Fig. 3a**). However, due to the presence of three chiral axis along with the interflavonyl

bonds, three rotamers are present with equal intensities of $^{1}$H NMR signals (**Fig. 3a**). Upon heating the solution to 90 $^{o}$C in one minute, interflavonyl bond isomerization occurs rapidly to give new sets of $^{1}$H signals (**Fig. 3b** red-colored peaks). We proposed that isomerization could occur through ortho-semiquinone anion radical intermediates facilitated in basic conditions or upon heating (**Fig. 3b and c**). We calculated the Gibbs free energies of four possible isomers of **CTL** and found that they have relatively similar free energies (**Fig. 3d),** in agreement with the formation of all these isomers in experiment. Which was further supported by the spin density distribution in CTL radical predicted by DFT (UM062x/6-311+G(d,p)), which shown that both C(2') and C(6') have comparable spin density **(Supplementary Fig. 83**).

With the success of homo-cross-coupling of luteolin, we pondered whether a similar homo-cross-coupling reaction could be extended to other flavones. We dissolved apigenin, diosmetin, chrysin, wogonin, 5,6-dihydroxyflavone, and genistein in alkaline water (pH 11.5). However, no desired coupling products were detected under the same conditions. Instead, only starting materials were recovered. No free radical signals were detected by EPR spectroscopy in the reaction solution, suggesting that they are insensitive to oxygen. These flavones lack catecholic groups preventing them from forming *ortho*-semiquinone anion radicals. In contrast, treating trihydroxyflavones containing catecholic B ring including 3′,4′-dihydroxyflavone, 3′,4′,5-trihydroxyflavone, 3′,4′,6-trihydroxyflavone and 3′,4′,7-trihydroxyflavone in alkaline water resulted in the formation of ortho-semiquinone anion radicals as detected by EPR spectra (**Supplementary Fig. 59-62**). However, there was little coupled reaction products detected (**Supplementary Fig. 5**). These observations suggested that these trihydroxyflavones are not sufficiently nucleophilic to accept the semiquinone radicals

generated from their oxidation. This agrees with the calculations by density functional theory which found that trihydroxyflavones have much lower nucleophilicity than luteolin (**Supplementary Fig. 6**). Hence, luteolin anion is unique among these flavones because of its high nucleophilicity and the ability to form *ortho*-semiquinone anion radicals, enabling it to undergo a coupling reaction.

*Hetero-cross coupling of flavones* When luteolin was mixed with excess apigenin (1:1.5 molar ratio), (Lu-(2′-6)-Ap, **2b**, was isolated in good yield (47%) together with a trace amount of Lu-(2′-8)-Ap, **2b′**, a triflavone (Lu-(2′-6)-Lu-(2′-6)-Ap (**3b**)), and a trace amount of **2a** (**Supplementary Fig. 7**). The structure of **2b** was confirmed by single crystal X-ray diffraction analysis to be desoxydicranolomin (**Fig. 4a**), a biflavone isolated from *Plagiomnium undulatum*[28]. Taken together, it became apparent that *a general rule for oxygen mediated oxidative coupling of two flavones is that one flavone is a radical precursor by forming ortho-semiquinone anion radicals, while the other flavone is a good nucleophile under the weakly basic reaction conditions*. This rule is valid for luteolin coupling with diosmetin (Di) (Lu-(2′-6)-Di, **2c,** with 65% yield, **Supplementary Fig. 8**), chrysin (Ch) (Lu-(2′-6)-Ch, **2d**, 46%, **Supplementary Fig. 9**), wogonin (Wo) (Lu-(2′-6)-Wo, **2e**, 85%, **Supplementary Fig. 10**), 5,6-dihydroxyflavone (Df) (Lu-(2′,7)-Df, **2f**, 57%, **Supplementary Fig. 11**) and Lu-(2′,8)-Df (**2f′**), and genistein (Ge) (Lu-(2′-6)-Ge (**2g,** 28%) and Lu-(2′-8)-Ge, **2g′**, 14%) (**Supplementary Fig. 12**).

Furthermore, when luteolin was mixed with trihydroxyflavones (TFL) with catecholic group on B ring (**1h-1j**) and 3′,4′-dihydroxyflavone (**1k,** DFL), luteolin became a nucleophile and **1h-1k** were the radical precursor yielding corresponding biflavones FL-(2′-6)-Lu (**2h-2k**, FL = TFL and DFL, **Supplementary Fig. 13-S16**) (**Fig. 4a**). Not surprisingly, **1h-1k** couple with other nucleophilic flavones such as apigenin, forming

175 FL-(2′-6)-Ap (**2l, 2m, 2n, 2o**) as the sole product (**Supplementary Fig. 17-20**). These
176 results broaden the scope of our reaction to diverse biflavones containing two different
177 monoflavones. There are many other feasible combinations of flavones and flavone
178 glycosides that can meet this simple requirement.

179

180 *Synthesis of hetero triflavonoids*. Our reaction can be extended to the synthesis of novel
181 triflavonoids by reacting **2a** (radical precursor) with nucleophilic flavones. These
182 triflavones share the same type of interflavonyl bonds with the general formula of Lu-(2′-
183 6)-Lu-(2′-6)-FL (FL = apigenin (**3b**), **Supplementary Fig. 21**) diosmetin (**3c**,
184 **Supplementary Fig. 22**), chrysin (**3d, Supplementary Fig. 23**), wogonin (**3e,**
185 **Supplementary Fig. 24**), 5,6-dihydroxyflavone (**3f. Supplementary Fig. 25**), and
186 genistein (**3g**, **Supplementary Fig. 26**) (**Fig. 5a**). The common features for these
187 compounds are the presence of atropisomers due to hindered rotation of the interflavonyl
188 bonds resulting in complex $^{1}$H and $^{13}$C NMR spectra. Remarkably when **2a** reacted with
189 trihydroxyflavones containing B-catecholic unit, it became a nucleophile and yielded
190 products FL-(2′-6)-Lu-(2′-6)-Lu (**3h**, **3i**, and **3j**) (**Fig. 5a**. Semi-prep-HPLC
191 chromatograms are shown in **Supplementary Fig. 27-S29**). Biflavones other than **2a**
192 could also be coupling partners allowing the synthesis of triflavones. For example, **2j** has
193 a catecholic unit serving as a radical precursor, and it is coupled with nucleophilic
194 apigenin to form FL-(2′-6)-Lu-(2′-6)-Ap, **3k,** as a sole product (**Fig. 5b and**
195 **Supplementary Fig. 30**). **3k** is a unique triflavone containing three different monomeric
196 flavone units. These triflavones all exist as a mixture of atropisomers that could be
197 separated by HPLC (**Supplementary Fig. 31-S32**) but they isomerize over time and show
198 complex $^{1}$H NMR spectra (**Supplementary Fig. 34-S45**).

*Key factors influencing the reaction outcome*. It is well-known that under alkaline conditions, flavonoids containing catechol moieties are sensitive to oxidation forming semiquinone radical intermediates. A computational study on neutral flavones also suggested that the presence of catecholic units increases the radical stability through H-bonds formation and favors hydrogen atom abstraction.[29] However, the fates of these radicals were unclear and they are not harnessed for synthetic purposes, likely due to the formation of complex end-products. Our discovery is counter-intuitive and thus warrants an in-depth study on the key factors influencing the reaction outcome so that we can rationally maximize the yield and selectivity for synthetic use. These factors include pH, counter cations, and oxygen availability in the solution.

*A) Optimal reaction pH*. Oxidative cross-coupling of two luteolin occurs in a narrow pH range from 9.5 to 12.5, with optimal pH at 11.5 (**Supplementary Fig. 46A**) and the yield dropped quickly at pH above 13.0. For the cross-coupling reaction between two different flavones, the pH profile is dependent on individual flavones with an optimal pH of 11.0-11.5, except for 5,6-dihydroxyflavone, which has an optimal pH of 10.0 (**Supplementary Fig. 46B-J**). This observation suggested that the optimal pH of the reaction is determined by the different p$K_a$ values of flavones. Similar pH profiles were found for oxidative coupling reactions between **2a** with flavones (**Supplementary Fig. 47**). The p$K_a$ values of the luteolin have been reported previously.[30] However, p$K_a$ is highly dependent on solvents and ionic strength. In addition, it is important to determine the positions of deprotonations corresponding to specific p$K_a$ values. Given the fact that luteolin can be oxidized at basic pH, the colorimetric p$K_a$ measurements are subject to interference by the luteolin oxidation products. Therefore, we determined the p$K_a$ values of specific phenolic protons by $^{13}$C NMR spectra of luteolin measured under argon [31]

(**Supplementary Fig. 48-54**). The first deprotonation occurred at C(7)-OH with p$K_{a1}$ of 8.00. This value is about two units larger than literature values (~ 6.0) (*21*). Our value agrees with the observation that luteolin has poor solubility in water or slightly basic aqueous solution. The p$K_{a2}$ was found at 8.93 (C(4′)-OH). The p$K_{a3}$ and p$K_{a4}$ are close to each other at 12.78 (C(3′)-OH) and 13.03 (C(5)-OH), respectively (**Fig. 6a**). Therefore, under the optimal reaction pH, luteolin (abbreviated as $LuH_4$, instead of Lu to illustrate the degree of deprotonation) dianion ($LuH_2^{2-}$) is the dominant species. To probe the presence of luteolin radical anions, we measured the EPR spectra of air-saturated luteolin solutions in different pH and found that oxidation of $LuH_2^{2-}$ only occurred significantly at pH above 9.5 (**Supplementary Fig. 55**). This suggested that the oxidation of $LuH_2^{2-}$ can only happen at pH at or greater than p$K_a$ of $LH_2^{\bullet-}$ so that electron transfer-induced deprotonation can occur simultaneously:

$$LuH_2^{2-} + O_2 \rightarrow LuH_2^{\bullet-} + O_2^{\bullet-} \quad (1)$$

$$HO^- + LuH_2^{\bullet-} \rightarrow LuH^{\bullet 2-} + H_2O \quad (2)$$

Thus, the p$K_a$ value of the unobserved intermediate [$LuH_2^{\bullet-}$] dictates the lower limit of the pH range of the reaction. From the EPR signal intensity plots against different pH the $pK_a$ value of $LuH_2^{\bullet-}$ is estimated to be 9.65 (**Fig. 7a**), which is close to the lower pH limit of the reaction. The $LuH^{\bullet 2-}$ radicals detected by EPR had the same hyperfine coupling patterns (**Fig. 6b**) that was reported in the literature (*21*). The spin density of $LuH^{\bullet 2-}$ map shows that C2' has the highest density (**Fig. 6c**).

The *ortho* semiquinone radicals of other flavones with catecholic B rings were detected, and the C2's also have the highest spin density (**Supplementary Fig. 56-S59**) in agreement with the fact that C2' is the major site of the coupling reaction. At higher pH

(> 12.5), the $LuH^{\bullet 2-}$ radical signal is depleted and a new radical species was detected featuring a doublet of doublets splitting pattern (**Supplementary Fig. 60**). To pinpoint the nature of the new radical species, the EPR spectra were measured under $^{17}O$ labelled oxygen and water, respectively. We found that $^{17}O_2$ did not alter the EPR peak splitting patterns (**Fig. 6d**). On the other hand, the EPR spectrum of luteolin (pH 12.5) in $^{17}O$-water (30% isotope purity) resulted in a new signal, a sextet due to the hyperfine coupling with $^{17}O$, suggesting that $H^{17}O^-$ addition to $C_{2'}$ position (**Fig. 6d** and **Supplementary Fig. 61**). We propose that $LuH^{\bullet 2-}$ undergoes dismutation to give an *ortho*-quinone intermediate (**Fig. 6e**), which can react with hydroxide at high pH resulting in the observed $LuOH^{\bullet 2-}$ radical, which is detrimental to the coupling reaction.

Based on these observations, we propose a coupling reaction mechanism shown in **Fig. 7a**. In alkaline water, luteolin undergoes deprotonation at C(7)-OH and catecholic protons to give $LuH_2^{2-}$, which undergoes single electron transfer to oxygen, coupled by deprotonation, to give $LuH^{\bullet 2-}$, under oxygen limiting conditions (simply without stirring). This radical anion couples with luteolin dianion, which is the dominant species under the reaction conditions. Computational results suggested that the C(6) of luteolin dianion has lower averaged local ionization energy (ALIE, Fig. S82) values than C(8) and thus C(6) is a preferred reaction site, resulting in 2′-6 biflavone as the major product. Furthermore, our computational results also show that 2′-6 isomer dicranolomin (**2a**) is more stable than 2′-8 isomer philonotisflavone (**2a′**) by 1.3 kcal/mol (**Fig. 7c**). Dicranolomin (**2a**) has two catecholic moieties. Remarkably, its reaction products with flavone monomers are highly regiospecific on the unreacted catecholic moiety (IIB), suggesting that semiquinone radicals from IIB are involved (**Fig. 7a**). The EPR spectrum of the *ortho*-semiquinone anion radical of **2a** (**Supplementary Fig. 62**) shows complicated signals

due to multiple radical species, including the semiquinone formed on IIB with $a_{H1}$ of 0.285 mT (**Supplementary Table 3**). The other radical may reside in the IB ring with $a_{H1}$ of 0.43 mT (**Supplementary Table 3**). The semiquinone radical at IB ring did not participate in coupling reaction, as linear trimer Lu-Lu-FL, instead of the branched trimer, is observed and isolated.

*B) Impact of counter cations in the coupling reaction*. For two dianions ($LuH^{\bullet 2-}$ and $LuH_2^{2-}$) to reaction, charge repulsions have to be overcome possibly by ion pairing with counter cation. Therefore, we examined the effects of different counter cations on the reaction; we found that tetramethylammonium ($Me_4N^+$, added as $Me_4NOH$) gave the lowest yield (< 20%). Lithium performed better but not as good as cesium, sodium and potassium (~80%) (**Fig. 7c**). These results suggested that the counter cations not only offset the anionic charges but might also facilitate the reaction through bridging both coupling partners closer to each other with weak coordination interactions. In this regard, a small lithium ion is not as effective as larger alkali metal ions. In aqueous solution, alkali metal ions are present as hydrates, and the coordination bonds with phenolates of the luteolin dianions shall be fairly weak and dynamic.

*C) Impact of oxygen availability*. Although ortho-semiquinone anion radical of luteolin has been observed previously, the end-products were found to be complex and were not characterized, likely due to overoxidation by excessive oxygen in the solution. The positive outcome of our case is likely due to limiting oxygen and by conducting the reaction unstirred, which is a counter-intuitive result. We compared the reaction dynamics of alkaline luteolin solution in two test tubes; one tube was magnetically stirred vigorously (so that oxygen is in excess supply) while the other tube was not stirred

295 (oxygen availability is dependent on the diffusion of the gas phase oxygen into solution).
296 The coupled products in the stirred tube could not be detected after 4 hours, while in the
297 unstirred tube, both **2a** and **3a** showed two major products after 10 hours
298 (**Supplementary Fig. 63-64**). The air saturated water has a dissolved oxygen
299 concentration of about 256 μM and its concentration is lower in alkaline water[32]. At the
300 beginning of the reaction, the dissolved oxygen in both tubes was quickly depleted by
301 reacting with $LH_2^{2-}$. However, stirring replenishes the dissolved oxygen, which undergoes
302 radical coupling reaction with $LH^{\bullet 2-}$ leading to overoxidation. In the unstirred tube, such
303 a reaction is prevented due to depleted oxygen and the slow diffusion of the gaseous
304 oxygen to the undisturbed solution which will prevent product formation over time
305 (**Supplementary Fig. 65-66**). Therefore, limiting oxygen availability is a key factor for
306 oxygen mediated oxidative coupling reaction of flavones.

307 Other oxidants may also trigger oxidative coupling of luteolin. For example, DPPH (2,2-
308 diphenyl-1-picrylhydrazyl) was able to trigger reaction between luteolin and cysteine
309 ethyl ester to form a low yield 1,4-thiazine derivative of luteolin through 2'-position (B-
310 ring) via sulfur and at the 3'-position via nitrogen.[33] We found that when luteolin was
311 treated radical precursor 2,2'-azobis(2-amidinopropane) dihydrochloride (AAPH),
312 luteolin reacted with radicals generated from AAPH and resulted in isolation of a lactone
313 derivative of luteolin via its B ring (C-2' and C-3')[34]. In both cases, the reactions were
314 likely via a radical-radical mechanism. In contrast, the coupling reactions we reported
315 herein involved A-ring of flavones as a nucleophiles.

316 *Contrasting bioactivity of the flavonoids dimers and trimers*. It has been suggested that
317 moss utilizes a large amount of bioresource in the synthesis of luteolin dimers and trimers,
318 because of the need to defend against the microbial stress endured by the moss while

319 growing on rotting wood in wet forests[35]. To test this hypothesis, we measured the
320 antifungal activity of luteolin, dicranolamin (**2a**), and distichumtriluteolin (**3a**) using
321 *Aspergillus niger* as a model fungus (**Supplementary Fig. 67**). Dicranolomin (**2a**) and
322 distichumtriluteolin (**3a**) inhibit the growth of *A. niger* with $IC_{50}$ of 0.86 μM and 0.96 μM,
323 respectively, which is comparable to that of amphotericin B ($IC_{50}$ of 0.50) in a dose-
324 dependent manner. Notably, dimer **2a** shows slightly higher activity than trimer (**3a**).
325 Plant flavonoids protect the plant from being eaten by insects by inhibiting digestive
326 enzymes such as α-amylase and α-glucosidase. We measured the activity of selected
327 flavone dimers and trimer (**2a**-**2f**, **3a**-**3f**) in inhibiting α-amylase and α-glucosidase
328 (**Supplementary Fig. 68-78**) and found that dimers **2a** and **2b** show comparable (**2a**) or
329 even higher (**2b**) activity than acarbose, an antidiabetic drug. Molecular docking by using
330 the crystal structure of a pancreatic α-amylase with acarbose complex[36] found that flavone
331 oligomers (**2a**, **2b**, **3a**) are located at the active center while that of luteolin is not, which
332 might explain why luteolin has no activity. The active site region of α-amylase is a V-
333 shaped depression located at the carboxyl end of Glu233, Asp300, and Aspl97. The
334 molecular shape of **2a a**nd **2b** (**Supplementary Fig. 79 and 81**) happens to be V-shaped
335 (similar to that of acarbose in **Supplementary Fig. 80**) and fits nicely in depression with
336 one B-ring near the catalytic active groups and form hydrogen bonding through the
337 catecholic group with Glu233, Asp300, and Aspl97.

338 In summary, we have demonstrated that by judiciously controlling the reaction
339 conditions, the oxygen mediated oxidative coupling reaction can be achieved for synthetic
340 purpose and that the reaction scope may be extended for the facile construction of other
341 complex molecules by coupling other naturally occurring phenolic compounds such as
342 stilbenoids and auronoids.

343

344 ## References


1. Gaspar, A., Matos, M. J., Garrido, J., Uriarte, E., Borges, F. Chromone: a valid scaffold in medicinal chemistry. *Chem. Rev*. **114**, 4960–4992 (2014).
2. Reis, J., Gaspar, A., Milhazes, N., Borges, F. Chromone as a privileged scaffold in drug discovery: recent advances. *J. Med. Chem*. **60**, 7941–7957 (2017).
3. Sarkhosh-Khorasani, S. and Hosseinzadeh, M. The effect of grape products containing polyphenols on C-reactive protein levels: a systematic review and meta-analysis of randomised controlled trials. *Br. J. Nutr.* **125** (11), 1230-1245 (2021).
4. Ried, K., Fakler, P., Stocks, N. P. Effect of cocoa on blood pressure. *Cochrane Database of Systematic Reviews* Article Number CD008893, DOI10.1002/14651858.CD008893.pub3 (2017).
5. Hussain, T., Tan, B., Murtaza, G., Liu, G., Rahu, N., Kalhoro, M. S., Kalhoro, D. H., Adebowale, T. O., Mazhar, M. U., Rehman. Z. U. Flavonoids and type 2 diabetes: Evidence of efficacy in clinical and animal studies and delivery strategies to enhance their therapeutic efficacy. *Pharmacol. Res* 152 Article Number 104629 (2020).
6. Scarmeas, N., Anastasiou, C. A., Yannakoulia, M. Nutrition and prevention of cognitive impairment. *Lancet Neurol.* **17** (11) 1006-1015 (2018).
7. Patel, T. S., Crutchley, R. D., Tucker, A. M., Cottreau, J., Garey, K. W. Crofelemer for the treatment of chronic diarrhea in patients living with HIV/AIDS. *HIV Aids-Research and Palliative Care*. **5**, 153-162 (2013).
8. Colletti, A., Sangiorgio, L., Martelli, A., Testai, L., Cicero, A. F. G., Cravotto, G. Highly active cranberry's polyphenolic fraction: New advances in processing and clinical applications. *Nutrients* **13**(8), Article Number2546, DOI10.3390/nu13082546 (2021).
9. Nallusamy, S., Mannu, J., Ravikumar, C., Angamuthu, K., Nathan, B., Nachimuthu, K., Ramasamy, G., Muthurajan, R., Subbarayalu, M., Neelakandan, K. Exploring phytochemicals of traditional medicinal plants exhibiting inhibitory activity against main protease, spike glycoprotein, RNA-dependent RNA polymerase and non-structural proteins of SARS-CoV-2 through virtual screening. *Front. Pharmacol.* 12, Article Number 667704 DOI10.3389/fphar.2021.667704 (2021).
10. Suzuki, A. Cross-coupling reactions of organoboranes: an easy way to construct C–C bonds (Nobel Lecture). *Angew. Chem. Int. Ed*. **50**, 6722–6737 (2011).
11. Malapit, C. A., Bour, J. R., Brigham, C. E., & Melanie S. Sanford, M. S. Base-free nickel-catalysed decarbonylative Suzuki–Miyaura coupling of acid fluorides *Nature* **563**, 100–104 (2018).
12. Ullmann, F., Bielecki, J. (1901). Ueber synthesen in der biphenylreihe. *Chemische Berichte*. **34** (2): 2174–2185 (1901).
13. Miyaura, N., Suzuki, A. Palladium-catalyzed cross-coupling reactions of organoboron compounds. *Chem. Rev*. **95** (7), 2457–2483 (1995).
14. Ndoile, M. M., Heerden, F. R. V. Total synthesis of ochnaflavone. *Beil. J. Org. Chem.***9**, 1346-1351 (2013).
15. Park, H-I., Si, C-L., Chen, J. Total synthesis of amentoflavone. *Med chem* **5**, 467-469 (2015). doi:10.4172/2161-0444.1000302.
16. Moon, T. C., Quan, Z., Kim, J., Kim, H. P., Kudo, I., Murakami, M., Park, H., Chang, H. W. Inhibitory effect of synthetic C-C biflavones on various phospholipase A(2)s activity. *Bioorg. Med. Chem.* **15**, 7138–7143 (2007).
17. Zimmerman, J. B., Anastas, P. T., Erythropel, H. C., Leitner, W. Designing for a green chemistry future. *Science* **367**, 397–400 (2020).
18. Geiger, H. &T. Seeger, T. Triflavones and a biflavone from the moss Rhizogonium distichum. *Z. Naturforsch*. **55c**, 870-873 (2000).

19. Cotelle, N., Bernier, J-L., Catteau, J-P., Pommery, J. Wallet, J-C., Gaydou, E. M. Antioxidant properties of hydroxy-flavones. *Free Radic. Biol. Med*. **20** (1) 35-43 (1996).
20. Kuwabara, K., Sakurai, Y., Sanuki, H., Morimoto, C., Li, Y., Miyake, Y., Kanaori, K., Tajima, K. Application of a stopped-flow EPR method for the detection of short-lived flavonoid semiquinone radicals produced by oxidation using $^{15}$N-labeled nitrosodisulfonate radical (Fremy's Salt). *Appl. Magn. Reson.* **49**, 911–924 (2018).
21. Ramešová, Š., Tarábek, R. S. J., Deganoca, I. The oxidation of luteolin, the natural flavonoid dye. *Electrochim. Acta* **110**, 646– 654 (2013).
22. We use this nomenclature to name flavone dimers and oligomers. For example, Lu-(2'-6)-Lu represents luteolin (Lu) dimer linked by through the C(2') of the first luteolin with the C(6) of the second luteolin.
23. Wang, H., Liu, S., Wang, T., Liu, H., Xu, X., Chen, K., Zhang, P. The moss flavone synthase I positively regulates the tolerance of plants to drought stress and UV-B radiation. *Plant Science* **298** 110591 (2020).
24. Waterman, M., Nugraha, A., Hendra, R., Ball, G., Robinson, S., Keller, P. Antarctic moss biflavonoids show high antioxidant and ultraviolet-screening activity. *J. Nat. Prod*. 80(8), 2224-2231 (2017).
25. Covington, C. L., Junior, F. M. S., Silva, J. H. S., Kuster, R. M., de Amorim, M. B., Polavarapu, P. L. Atropoisomerism in biflavones: the absolute configuration of (−)-agathisflavone via chiroptical spectroscopy. *J. Nat. Prod*. 79(10), 2530-2537 (2016).
26. Reisberg, S. H., Gao, Y., Walke, A. S., Helfrich, E. J. N., Clardy,J., Baran, P. S. Total synthesis reveals atypical atropisomerism in a small-molecule natural product, tryptorubin A. *Science* **367**, 458–463 (2020).
27. Geiger, H., Voigt, A., Seeger, T., Zinsmeister, H.-D., López-Sáez, J.-A., Pérez-Alonso, M. J., Negerúela, A. V. Cyclobartramiattriluteolin, a unique triflavonoid from *Bartramia stricta*. *Phytochemistry* **39**(2), 465-467 (1995).
28. Rampendahl, C., Seeger, T., Geiger, H., Zinsmeister, H. D. The biflavonoids of *Plagiomnium undulatum Phytochemistry* **41**(6), 1621-4 (1996).
29. Leopoldini, M., Pitarch, I. P., Russo, N., Toscano, M. Structure, conformation, and electronic properties of apigenin, luteolin, and taxifolin antioxidants. A first principle theoretical study. J. Phys. Chem. A. 108 (1), 92-96 (2004).
30. Favaro, G., Clementi, C., Romani, A., Vickackaite, V. Acidichromism and ionochromism of luteolin and apigenin, the main components of the naturally occurring yellow weld: A spectrophotometric and fluorimetric study. *J Fluoresc* **17**, 707–714 (2007).
31. Agrawal, P., Schneider, H. Deprotonation induced $^{13}$C NMR shifts in phenols and flavonoids *Tetrahedron Lett.* **24** (2) 177-180 (1983).
32. Xing, W., Yin, M., Lv, Q., Hu, Y., Liu, C., Zhang, J. Oxygen solubility, diffusion coefficient, and solution viscosity, Editor(s): W. Xing, G. Yin, J. Zhang. Rotating Electrode Methods and Oxygen Reduction Electrocatalysts. Elsevier, 2014, Pages 1-31. ISBN 9780444632784.
33. Masuda, T., Nojima, S., Miuraa, Y., Honda, S., Masuda, A. An oxidative coupling product of luteolin with cysteine ester and its enhanced inhibitory activity for xanthine oxidase. *Bioorg. Med. Chem. Lett.* **25**(16), 3117-9 (2015).
34. Lin,Y., Yang, X., Wu, Z., Sun, H., Huang, D., Sun, Zh. A newly synthesized flavone from luteolin escapes from COMT-catalyzed methylation and inhibits lipopolysaccharide-induced inflammation in RAW264.7 macrophages via JNK, p38 and NF-κB signaling pathways. *J. Microbiol. Biotechnol.* **32**(1), 15–26 (2022).
35. Geiger, H., Seeger, T., Zinsmeister, H. D., Frahm, J. R. The occurrence of flavonoids in arthrodontous mosses—an account of the present knowledge. *J. Hattori Bot. Lab*. **83**, 273-308 (1997).
36. Qian, M., Haser, R., Buisson, G., Duee, E., Payan, F. The active center of a mammalian alpha-Amylase. Structure of the complex of a pancreatic alpha-amylase with a carbohydrate inhibitor refined to 2.2 Å resolution. *Biochemistry* **33**, 6284-6294 (1994).


## Acknowledgements:

We thank Dr Yukio Mizuta of JEOL Corporate (Japan) for help in simulating the EPR spectra of luteolin and dicranolomin radical anions.

The research work was supported by Singapore Ministry of Education grant R160-000-B04-114 and National University of Singapore (Suzhou) Research Institute (NUSRI) via a grant under Peak of Excellent (POE) in Food Science and Technology.

**Author contributions:**

Conceptualization: XY and DH.

Data curation: XY, SHML, JL, HT, JYHT, KD, YZ, XW, MS, ZS, FL, FZ, TW, Ji'en Wu.

Formal Analysis: XY and DH.

Funding acquisition: DH.

Investigation: Experimental: XY, SHML, JL, HT, JYHT, KD, YZ, XW, MS, and ZS; Computational: FL, FZ and KNH (DFT calculations of the Gibbs energies); TW, SHML, CS, and XY (spin densities of radicals).

Formal Analysis: XY and DH.

Project administration: DH.

Supervision: DH (experimental), KNH (Computational).

Writing – original draft: DH and XY.

Writing – review & editing: KNH, DH, XY, FL, ZS, SHML, JYHT, JW.

**Competing interests**: Authors declare that they have no competing interests.

**Data and materials availability**: All data are available in the main text or the supplementary materials.

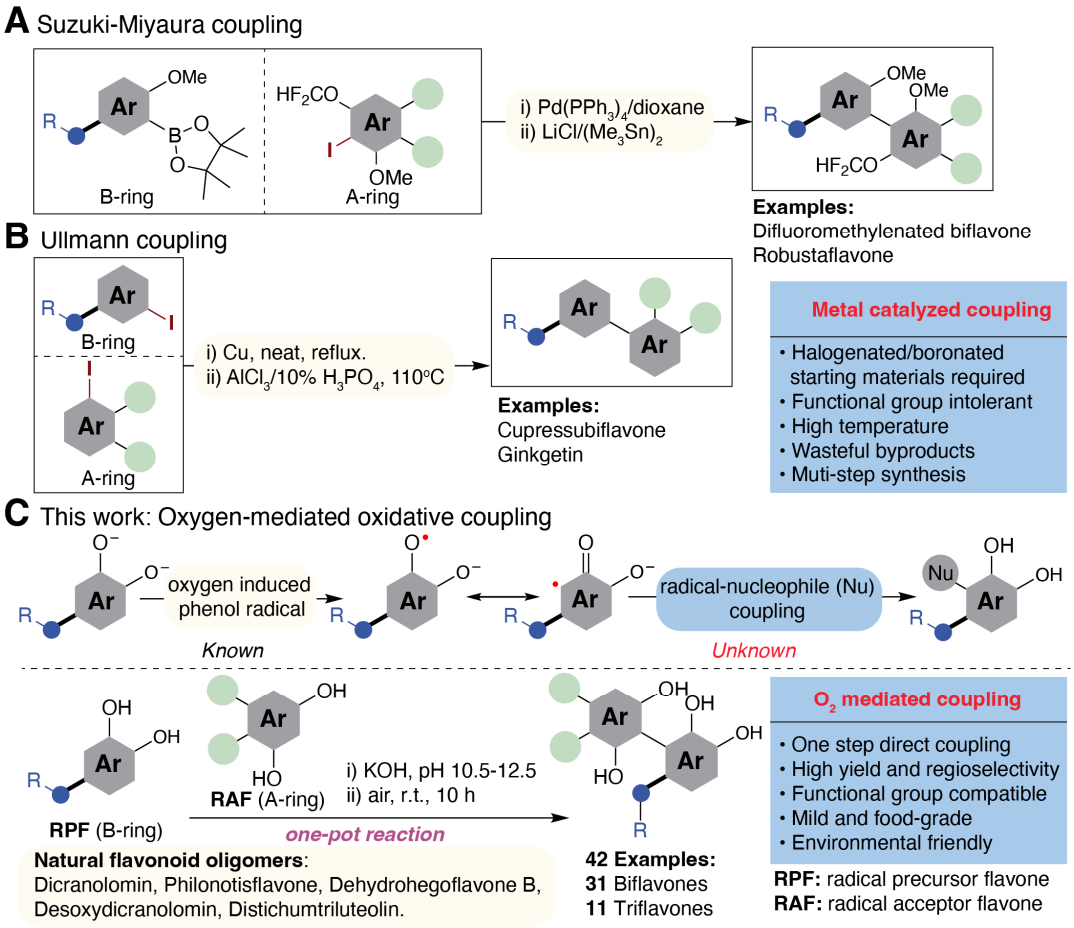


**Fig. 1 | Synthesis of nature-occurring and unnatural biflavones and triflavones. a**, Suzuki-Miyaura coupling reaction in the synthesis of biflavonoids. **b**, Ullmann coupling reaction in the synthesis of biflavonoids. **c,** this work: oxygen mediated oxidative coupling reaction in the synthesis of flavonoid oligomers; examples include 31 biflavones and 11 triflavones.

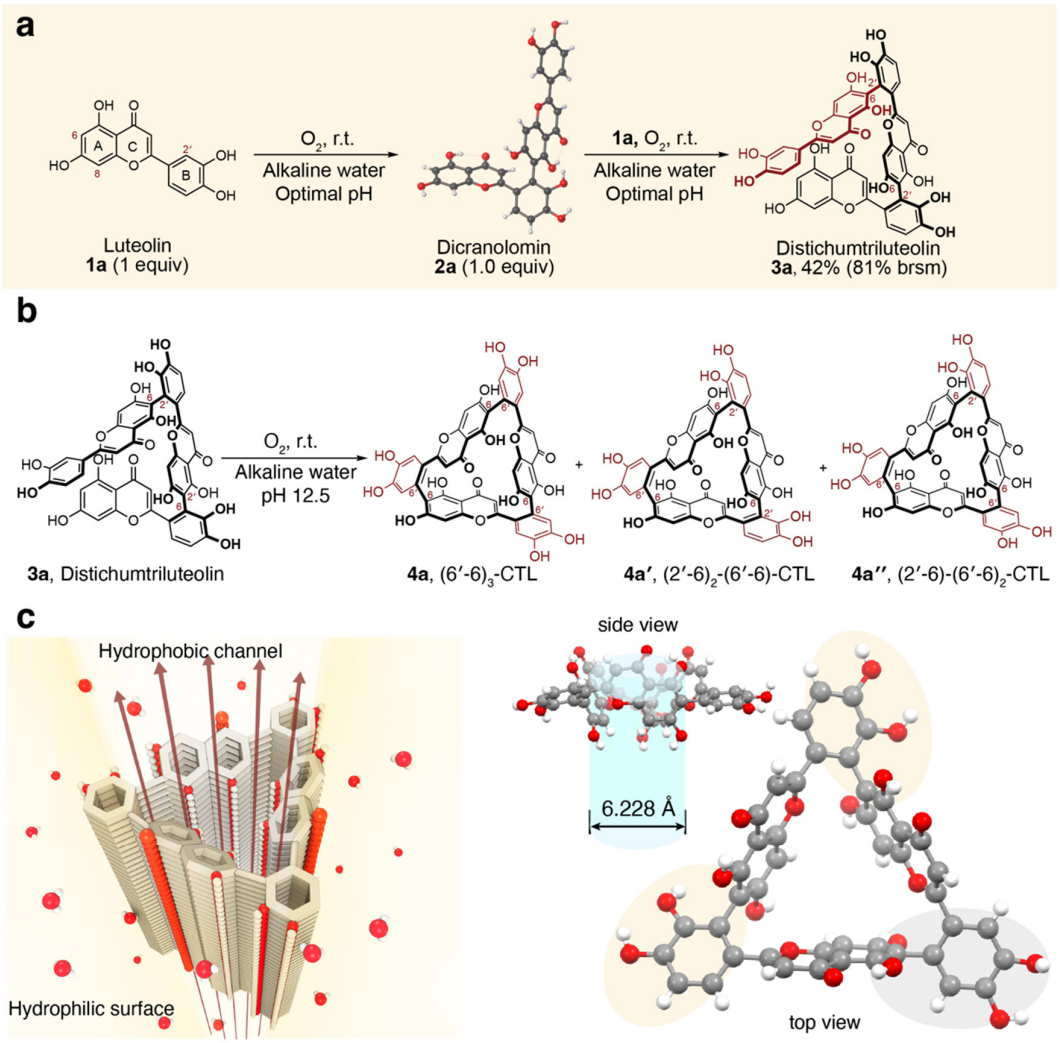


**Fig. 2 | Oxygen-mediated oxidative coupling of flavones. a,** Luteolin undergoes oxidative coupling reaction, under weakly alkaline water to major product dicranolomin (**2a**) and minor products, philonotisflavone (**2a′**, structure not shown), dehydrohegoflavone B (**2a″**) and distichumtriluteolin (**3a**), which could be obtained separately from the coupling of isolated **2a** and luteolin with 42% isolated yield. **b,** Intramolecular oxidative coupling **3a** proceeds to give different isomers cyclotriluteolin (**4a**, **4a′**, and **4a″**). **c,** the solid-state structure of one isomer **4a′** was determined by single-crystal X-ray diffraction.

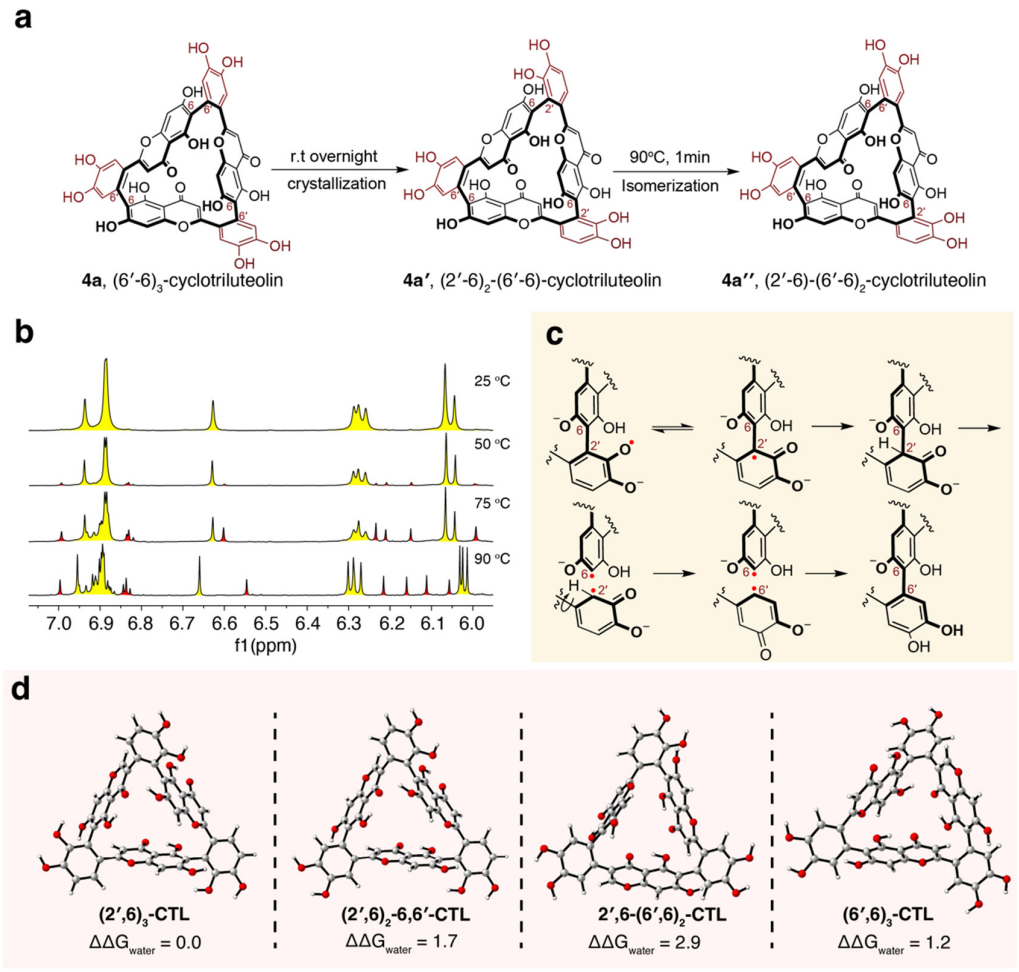


**Fig. 3 | a**, Ring rearrangement of cyclotriluteolin (CTL). **b,** Variable temperature NMR of 4a. **c,** Proposed intramolecular ring rearrangement of cyclotriluteolin. **d,** Calculated Gibbs free energies of cyclotriluteolin isomers. Calculations were performed at the M06-2X/6-311+G(d,p), SMD($H_2O$)//M06-2X/6-31G(d)SMD($H_2O$) level of theory. Energies are in kcal·mol$^{-1}$.

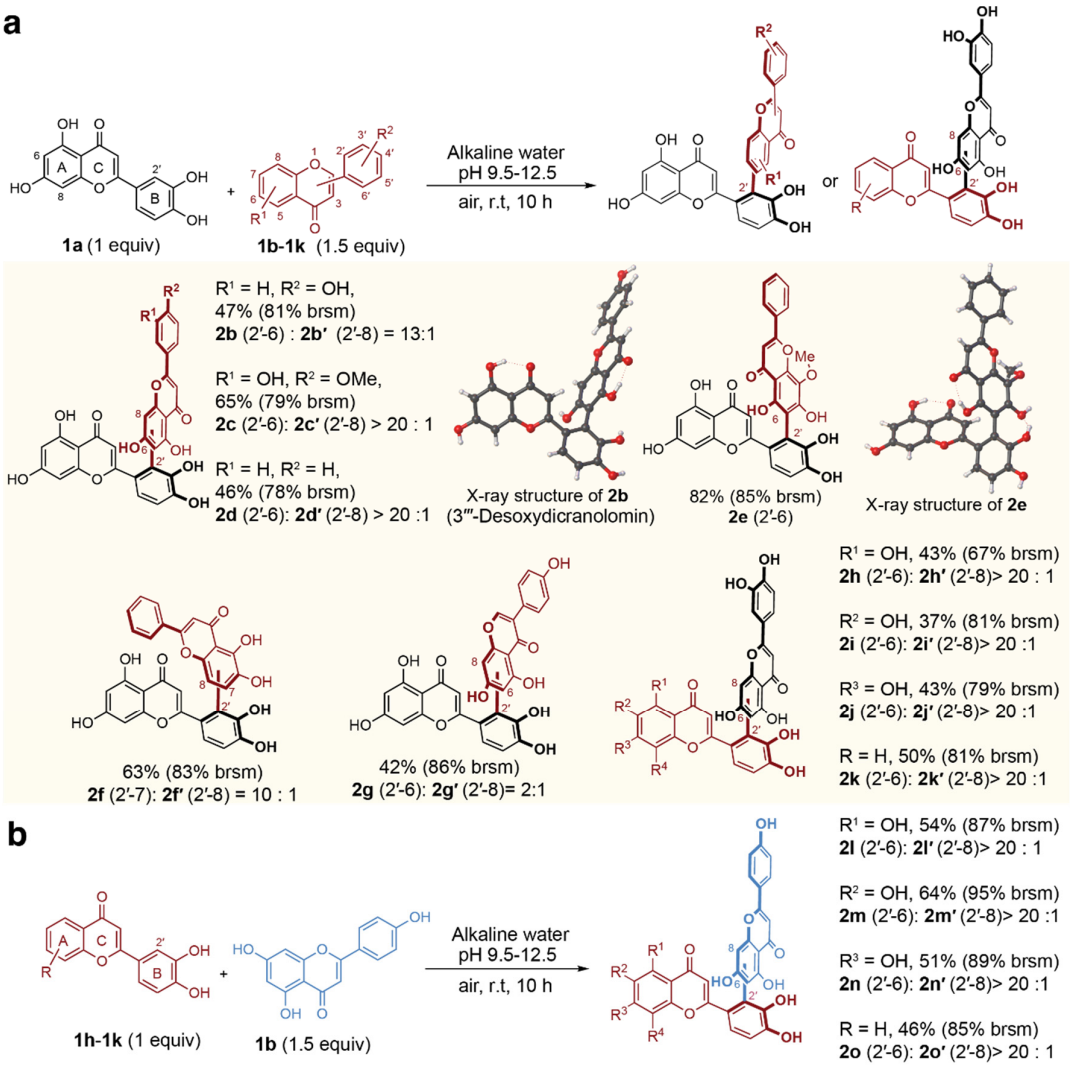


**Fig. 4 | The substrate scope of oxygen mediated cross-coupling of luteolin and flavones. a,** Luteolin as a radical precursor and acceptor. **b,** B-catechol flavones as a radical precursor. All yields were isolated and selectivity determined by HPLC analysis. brsm = yields based on the recovery of starting materials. R = H if not specified.

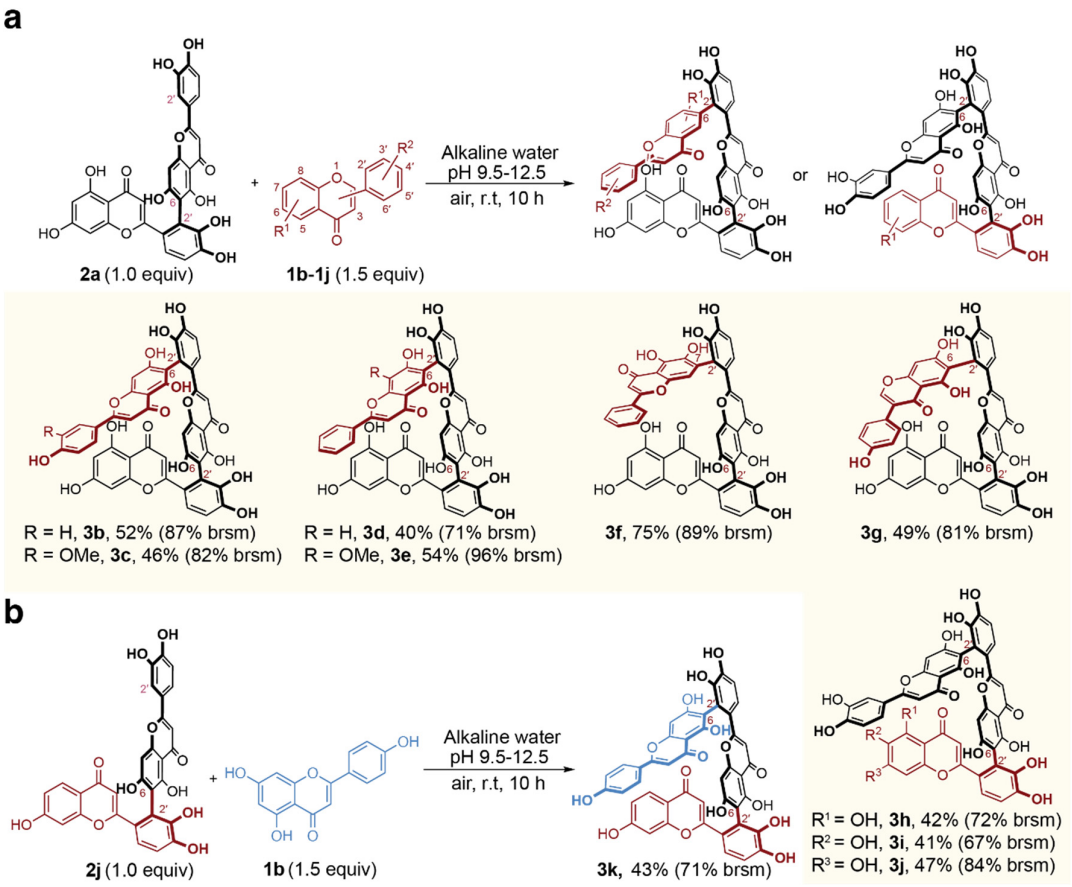


**Fig. 5 | The substrate scope of oxidative coupling for the synthesis of triflavones in alkaline water. a,** Dicranolomin as a radical precursor and acceptor. **b,** B-catechol biflavone as a radical precursor. All yields are isolated yields. brsm = yields based on the recovery of starting materials. R = H if not specified.

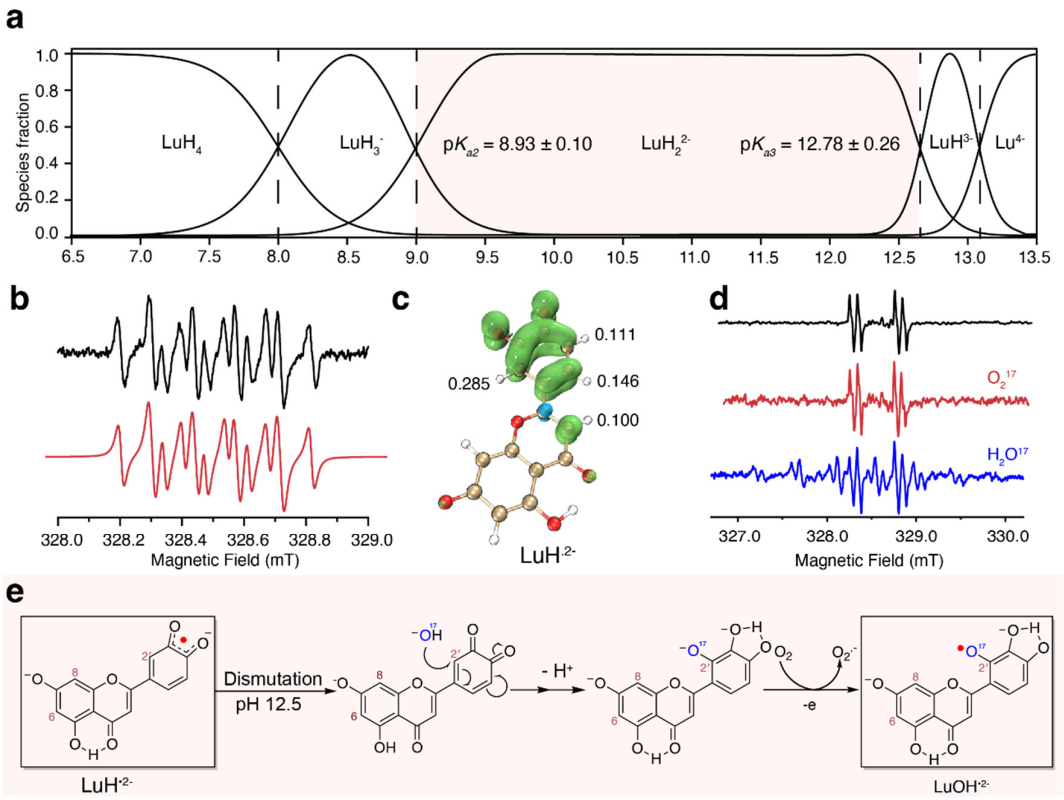


**Fig. 6 | pK$_a$ profile of luteolin and the radicals generated. a,** The distribution curve of luteolin species in aqueous solution $LuH_4$: luteolin, $LuH_3^-$: monoanion, $LuH_2^{2-}$: dianion, $LuH^{3-}$: trianion, and $Lu^{4-}$: tetraanion. **b,** Experimental (black) and simulated (red) EPR spectrum of $LuH^{\bullet 2-}$. **c,** Spin-density distribution in $LuH^{\bullet 2-}$ predicted with DFT (UM062X/6-311+G(d,p)). **d,** Experimental EPR spectrum of $LuOH^{\bullet 2-}$ in air-saturated $H_2O$ (Black), in $H_2O$ with 30% $^{17}O_2$-enriched molecular oxygen (red) and in 30% $^{17}O$ enriched water (blue). **e,** Proposed mechanism for the formation of $LuOH^{\bullet 2-}$.

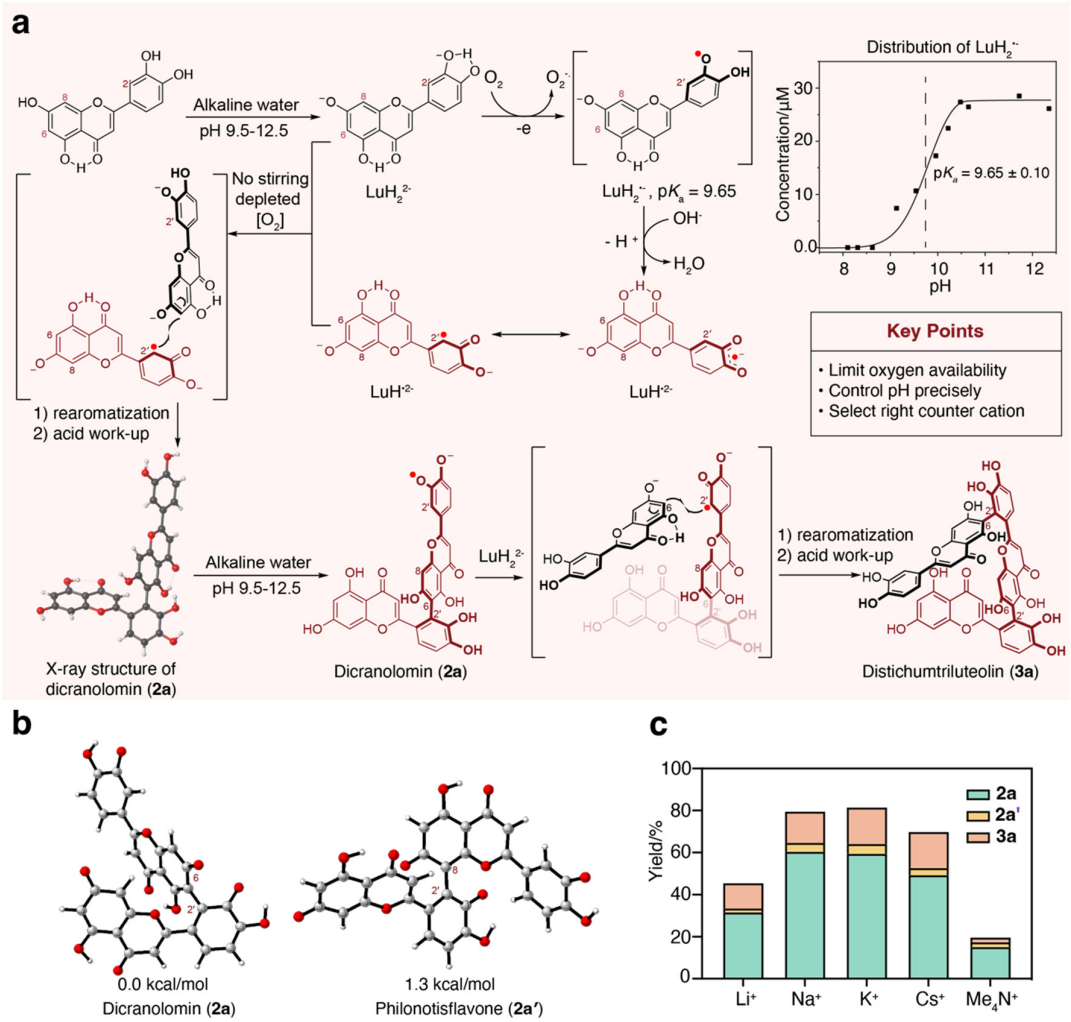


**Fig. 7 | Reaction mechanism and computational study of regioselectivity.** **a,** Proposed mechanisms for oxidative coupling reactions, counter-cations are omitted for clarity. **b,** Computed Gibbs energy difference between **2a** and **2a′**. **c,** the impact of counter-cations on the yields coupling reaction of luteolin.